ISSN: 2347-3487

PREPARATION, DIELECTRIC AND OPTICAL PROPERTIES OF Cr_2O_3 /PVC NANOCOMPOSITE FILMS

A. Hassen[a,b*], S. El-Sayed[a,b], W.M. Morsi[c], A.M. El Sayed[b,e]

[a] Department of Physics, Faculty of Science and Education, Al Khurma Branch, Taif University, Saudi Arabia.
[b] Department of Physics, Faculty of Science, Fayoum University, Fayoum 63514, Egypt
*Corresponding author: ash02@fayoum.edu.eg
[a] Department of Physics, Faculty of Science and Education, Al Khurma Branch, Taif University, Saudi Arabia.
[b] Department of Physics, Faculty of Science, Fayoum University, Fayoum 63514, Egypt
somyia.elsayed@yahoo.com
[c] Building Physics Institute, Housing and Building National Research Center, HBRC, Dokki, Giza 11511, Egypt
dr.wafaam@yahoo.com
[b] Department of Physics, Faculty of Science, Fayoum University, Fayoum 63514, Egypt
[e] Physics department, Faculty of Science, Northern Borders University, Arar 91431, KSA
ams06@fayoum.edu.eg

ABSTRACT

Chromium oxide (Cr_2O_3) nanoparticles were synthesized using a sol-gel method and mixed with polyvinyl chloride (PVC). Rietveld refinement of X-ray powder diffraction (XRD) patterns of the samples revealed that the crystal structure of Cr_2O_3 is rhombohedral with space symmetry group $R\bar{3}c$. Scanning electron microscopy images showed that the Cr_2O_3 nanoparticles are well dispersed on the surface of the PVC films. The dielectric permittivity (ε'), and ac conductivity (σ_{ac}) of pure PVC increased with adding Cr_2O_3 due to the formation of conductive three-dimensional networks throughout the nanocomposite films and interfacial polarizations. The optical energy band gap (E_g) of the films decreases with increasing Cr_2O_3 content. The refractive index dispersion of the nanocomposite films obeys the single oscillator model. The dispersion parameters are changed by incorporation of Cr_2O_3. The optical properties of PVC are influenced by addition of Cr_2O_3 nanoparticles.

Keywords:

Cr_2O_3 nanoparticles; polymer nanocomposites; dielectric properties; refractive index; optical dispersion.

Council for Innovative Research

Peer Review Research Publishing System

Journal: Journal of Advances in Physics

Vol 4, No.3

japeditor@gmail.com

www.cirjap.com

ISSN: 2347-3487

INTRODUCTION

In recent years, nanocomposite materials have received great interest for both industrial and academic applications [1,2]. Addition of a small amount of nanomaterial could improve the performance of polymeric materials because of their small size, large specific surface area, quantum confinement effects and strong interfacial interactions [3]. Polyvinyl chloride (PVC) is one of the most widely produced and used polymers globally [4]. PVC has high chemical resistance and can be used as a thermoplastic material [5-8]. PVC/graphite nanocomposites could be used for attenuation and electromagnetic interference shielding [9,10]. PVC/($Cd_{0.5}Zn_{0.5}O$) nanocomposites are reported to have high transparency, high UV-shielding efficiency and improved thermal stability compared with PVC [11]. Meanwhile, PVC/ZnO nanocomposites possess higher glass transition temperature, specific heat and thermal stability than those of pure PVC [12]. It has also been reported that PVC/ZnO-polyaniline hybrid nanocomposites protect iron from corrosion far more effectively than undoped PVC [13]. Numerous PVC-based nanocomposites with favorable properties have been developed, including PVC doped with Al_2O_3 [6], nano-TiO_2@Ag [7], reduced graphite nanosheets [8], graphene nanosheets [14], $CaCO_3$ nanoparticles [15], and multi-walled carbon nanotubes (MWCNTs) [16]. The electrical, mechanical, chemical, and thermal properties of these PVC nanocomposites have been examined, revealing that the properties of PVC were markedly improved by doping and its industrial applications could be broadened. We recently reported the optical and dielectric properties of cadmium oxide (CdO)/PVC nanocomposite films [17]. Addition of CdO nanoparticles to the PVC matrix improved both the optical and dielectric properties of the host polymer. α_a-relaxation process in pure and nano lead oxide (PbO) doped-PVC films was observed based on the temperature and frequency dependence of the electric modulus (M'')[18].

Chromium oxide (Cr_2O_3) nanoparticles are of interest for applications such as green pigments, wear resistance, thermal protection, digital recording systems, and chemical catalysts [19]. Cr_2O_3 nanoparticles have been prepared and characterized by many different researchers [20-25], with resulting particle size depending on the method of preparation. The crystal structure of Cr_2O_3 is rhombohedral with lattice parameters a = 4.95876 Å, and c = 13.594 Å and space symmetry group $R\bar{3}c$ [20,22]. With this background of multifunctionality, it is worthwhile investigating the ability of nanosized Cr_2O_3 to improve the optical properties of PVC, which has not been attempted to date.

Because of excellent control of stoichiometry, relative simplicity, and the general advantage of large-area deposition, the sol–gel technique and solution casting were chosen to prepare Cr_2O_3 nanoparticles and PVC/Cr_2O_3 nanocomposite films, respectively, in this work. The influence of Cr_2O_3 nanoparticles on the dielectric and optical properties of PVC are examined.

EXPERIMENTAL

Cr_2O_3 nanoparticles were synthesized by the sol-gel method. High-purity chromium triacetate ($Cr(C_2H_3O_2)_3$) and oxalic acid ($C_2H_2O_4$) were mixed in stoichiometric ratio and dissolved in double-distilled (*DD*) water with stirring for 2 h. The obtained sol was held in an oven at 100 °C for 8 h, cooled to 70 °C and stirred to obtain a gel that was then aged for 18 h at room temperature (*RT*). Finally, the gel was calcined at 400°C for 3 h to obtain Cr_2O_3 nanoparticles. The synthesized nanoparticles were added in different x (*wt.*%; x = 0, 0.2, 0.6, 0.8 and 1.2) to PVC according to the following equation:

$$x(wt.\%) = \frac{w_f}{w_f + w_p} \times 100 \qquad (1)$$

where w_f and w_p represent the weights of Cr_2O_3 and PVC, respectively. Nanocomposite films were prepared by casting as follows. PVC [Polymer Laboratories, Ltd. (Essex, UK)] (2.0 g) was dissolved in tetrahydrofuran [THF, Aldrich, Germany] (70 ml) with stirring for 1 h at *RT* until the polymer completely dissolved. Cr_2O_3 nanoparticles were added to the PVC solution in the appropriate ratio under vigorous stirring to prevent agglomeration. Finally, the aqueous mixtures were cast into Petri dishes and placed in an oven at 60 °C for 24 h in air. Care was taken to obtain homogenous samples of the same thickness. The obtained nanocomposite films of pure PVC and PVC loaded with Cr_2O_3 nanoparticles were then characterized.

The obtained Cr_2O_3 powder and films of pure PVC and PVC loaded with Cr_2O_3 nanoparticles were characterized by a range of techniques. X-ray diffraction (XRD) of Cr_2O_3 particles, PVC, and Cr_2O_3-doped PVC films was performed using a diffractometer (PANalytical,X'Pert PRO, Netherlands). High-resolution transmission electron microscopy (HR-TEM; JEM 2100, JEOL, Japan) was used to measure the crystalline size of the as-synthesized Cr_2O_3 particles. Scanning electron microscopy (SEM; Inspect S, FEI, Holland) images of pure PVC and the nanocomposite films were obtained. Film thickness was evaluated using a digital micrometer with an accuracy of ±0.001 mm. Dielectric measurements were performed by using a Hioki (Ueda, Nagano, Japan) model 3532 High Tester LCR, with capacitance measurement accuracy on the order of 1×10^{-4} pF. The temperature was measured with a T-type thermocouple having an accuracy of ±1°C. The dielectric permittivity ε' of each sample was calculated as $\varepsilon' = dC/\varepsilon_o A$; where C is the capacitance, d is the thickness of the sample, ε_o is the permittivity of free space, and A is the cross-sectional area of the sample. The measured ac conductivity values of Cr_2O_3/PVC composite films were calculated using the relation;

$$\sigma_{ac} = \omega \varepsilon_o \varepsilon' tan\delta = 2\pi f \varepsilon_o \varepsilon'', \qquad (2)$$

ISSN: 2347-3487

where ϖ is the angular frequency ($\varpi = 2\pi f$), f is the applied frequency, tan $\delta = \varepsilon''/\varepsilon'$, and ε'' is the dielectric loss factor. Optical characterization was carried out at *RT* using a UV-VIS-NIR spectrophotometer (Shimadzu UV-3600) in the wavelength range 230–800 nm with an accuracy of ±0.2 nm.

RESULTS AND DISCUSSION

Characterization

The Rietveld refinement of the XRD pattern of the as-synthesized Cr_2O_3 nanoparticles is shown in Figure 1(b). Cr_2O_3 crystallizes with a rhombohedral structure in space group $R\bar{3}c$. The lattice constants are a = 4.948(3) Å and c =13.581(0) Å. These parameters agree well with the results of a neutron diffraction study [26] and those reported in Refs. [20, 22, 27] for Cr_2O_3 nanoparticles. A HR-TEM image (Figure 1(a)) of the as-prepared Cr_2O_3 nanoparticles was taken to test the crystal size.

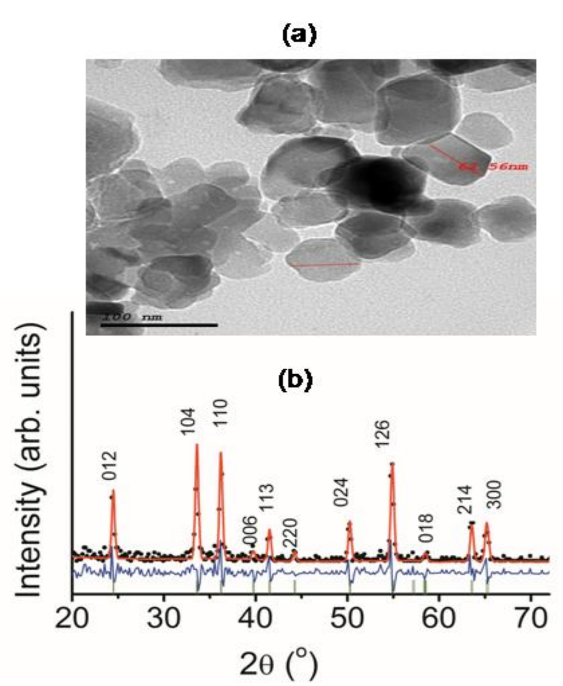

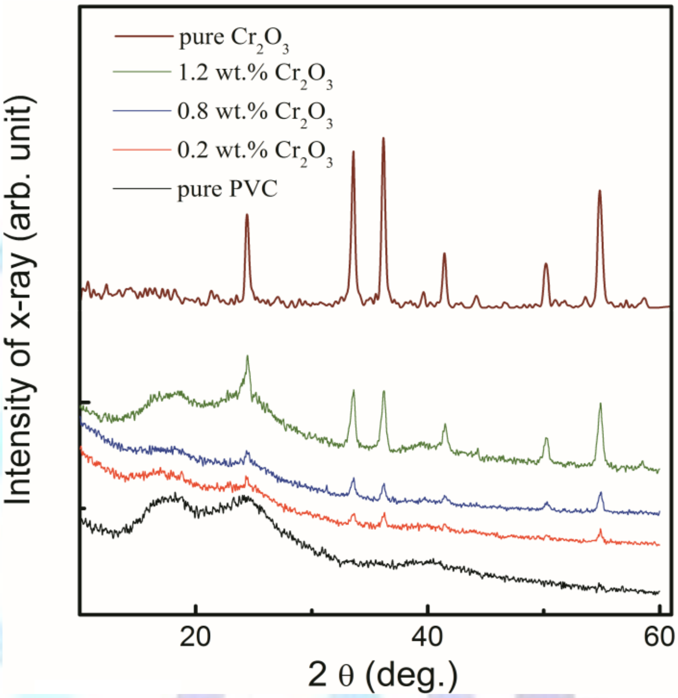

FIG. 1 (left): (a) HR-TEM image of Cr_2O_3 nanoparticles, and (b) XRD patterns of pure Cr_2O_3 nanoparticles, showing observed intensities (closed black circles), calculated intensities (red line), their difference (blue line), and the positions of the calculated reflections (green vertical bars).

FIG. 2 (right) : XRD patterns measured at room temperature of pure PVC, Cr_2O_3 nanoparticles and PVC loaded with Cr_2O_3 nanoparticles.

The average particle size of Cr_2O_3 was ~46 nm [28]. To highlight the differences between the XRD patterns of pure Cr_2O_3 and Cr_2O_3/PVC nanocomposite films, the XRD pattern of pure Cr_2O_3 is plotted along with those of pure PVC and the doped samples in Figure 2. The broad halo peak in the region of 15–35° observed for pure PVC indicates its amorphous nature [29, 30]. Comparing the XRD patterns of pure PVC and the as-prepared nanoparticles with those of the nanocomposite films reveals that Cr_2O_3 retains its rhombohedral structure even when it is dispersed in PVC. In addition, SEM was performed to examine the morphology and dispersion of Cr_2O_3 nanoparticles on the surface of the PVC films. Fig. 3(a-d) shows SEM images of pure PVC and some PVC/Cr_2O_3 nanocomposite films. Cr_2O_3 nanoparticles are well dispersed on the surface of PVC in all doped films.

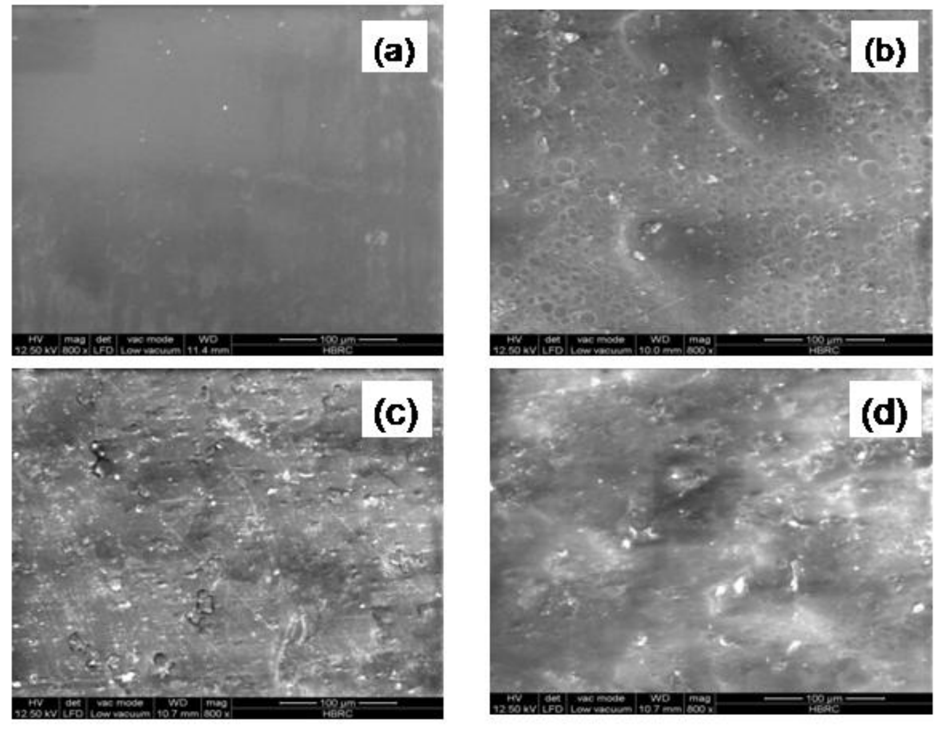

FIG. 3: SEM images of (a) pure PVC, (b) 0.2 *wt.%* Cr_2O_3-doped PVC, (c) 0.8 *wt.%* Cr_2O_3-doped PVC, and (d) 1.2 *wt.%* Cr_2O_3-doped PVC.

DIELECTRIC PROPERTIES

Dielectric Permittivity

Figure 4(a-c) represents the frequency dependence of ε' for a pure PVC film and PVC films loaded with Cr_2O_3 nanoparticles at different fixed temperatures. As seen, the ε' of the pure and doped films decrease with increasing field frequency because of decreases in the number of dipoles contributing to the polarization. The dielectric permittivities of Cr_2O_3–doped PVC films are significantly higher than that of the pure PVC. This can be attributed to interfacial polarization, which is difficult to observe because of the conductivity of the material. This polarization allows the dielectric permittivity to be high at low frequencies and high temperatures [31]. In addition, the effect of Cr_2O_3 nanoparticles on the dielectric permittivity of pure PVC is more pronounced than that of CdO [17]. This can be ascribed to the different chemical natures of these metal oxides.

ISSN: 2347-3487

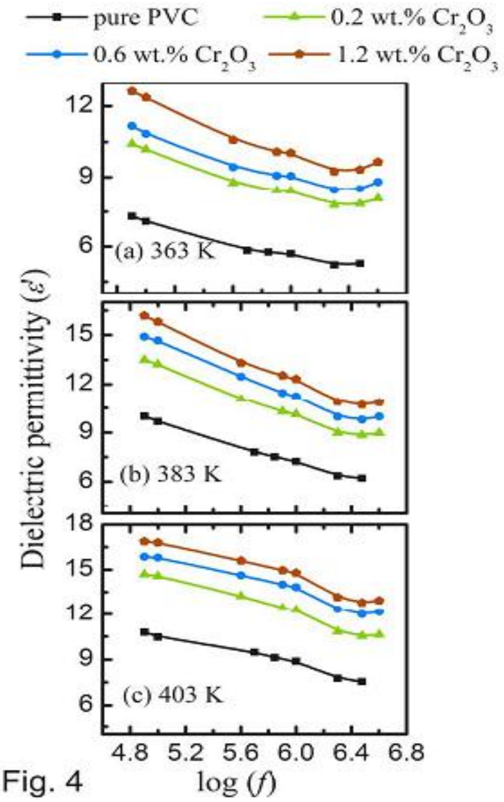

Fig. 4

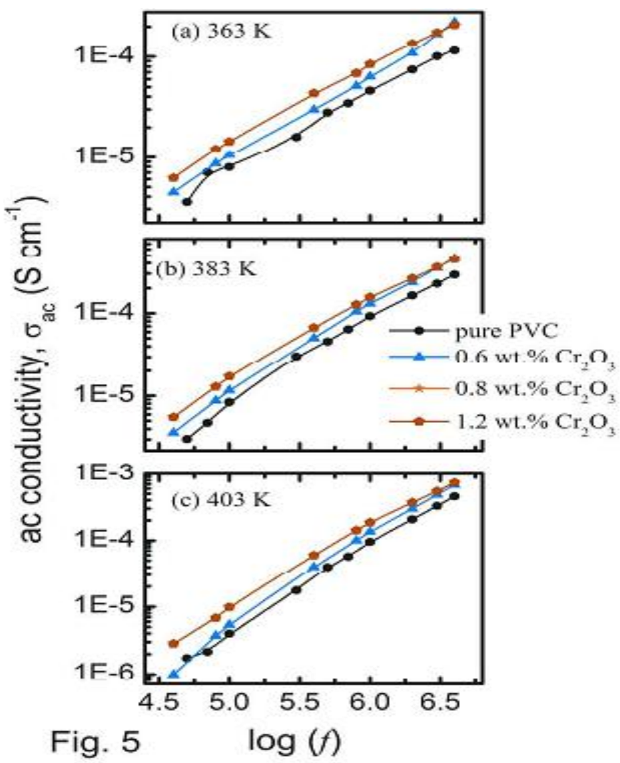

Fig. 5

FIG. 4: Frequency dependence of ε' for pure PVC films and PVC containing different *wt.*% Cr_2O_3 nanoparticles at different temperatures: (a) 363 K, (b) 383 K and (c) 403 K.

FIG. 5: Frequency dependence of σ_{ac} for pure PVC and PVC loaded with different Cr_2O_3 content at different temperatures: (a) 363 K, (b) 383 K and (c) 403 K.

AC Conductivity

Figure 5 (a-d) displays the dependence of σ_{ac} of the composite films on *f* at various temperatures. The increase in σ_{ac} with frequency and the weak temperature dependence indicate that the charge carriers are transported by hopping through defect sites along the chains [32]. The homogenous distribution of Cr_2O_3 nanoparticle, which confirmed from SEM, allows the formation of more number of conductive three-dimensional networks throughout the nanocomposite and assisting the charge carriers to hop from conducting clusters to neighbors. These observations agreed with the published data for different polymers and amorphous semiconductors [10, 14, 33, 34]. The difference between the values of σ_{ac} for 0.8 *wt.*% Cr_2O_3- and 1.2 *wt.*% Cr_2O_3-doped PVC is small.

The variation of the σ_{ac} with Cr_2O_3 content at different temperatures and frequencies are given in Table 1. Once again, σ_{ac} increases with the incorporation of Cr_2O_3 nanoparticles inside the PVC matrix. However, it is observed that the σ_{ac} values of 0.8 *wt.*% and 1.2 *wt.*% doped-PVC samples are very close to each other, may be the conductivity reaches its maximum. In addition, the values of σ_{ac} increase significantly with increasing the applied frequency rather than the increasing of temperature.

TABLE 1: The ac conductivity (σ_{ac} in units of $S.cm^{-1}$) values of the nanocomposite films at different temperatures and frequencies

	80 kHz			0.8 MHz			3.0 MHz		
Sample	323 K	363 K	393 K	323 K	363 K	393 K	323 K	363 K	393 K
0.2 *wt.*%	$4.76x10^{-7}$	$8.57x10^{-6}$	$6.20x10^{-6}$	$5.09x10^{-6}$	$4.8x10^{-5}$	$1.0x10^{-4}$	$8.03x10^{-6}$	$1.22x10^{-4}$	$3.48x10^{-4}$
0.6 *wt.*%	$2.5x10^{-7}$	$8.6x10^{-6}$	$6.7x10^{-6}$	$3.2x10^{-6}$	$5.1x10^{-5}$	$1.1x^{-4}$	$1.48x10^{-5}$	$1.70x10^{-4}$	$4.03x10^{-4}$
0.8 *wt.*%	$9.2x10^{-7}$	$1.2x10^{-5}$	$1.03x10^{-5}$	$8.1x10^{-6}$	$6.8x10^{-5}$	$1.4x10^{-4}$	$1.20x10^{-5}$	$1.75x10^{-4}$	$4.52x10^{-4}$
1.2 *wt.*%	$9.24x10^{-7}$	$1.2x10^{-5}$	$1.0x10^{-5}$	$8.1x10^{-6}$	$6.8x10^{-5}$	$1.4x10^{-4}$	$1.22x10^{-5}$	$1.76x10^{-4}$	$4.53x10^{-4}$

ISSN: 2347-3487

Electric Modulus

In composite polymeric materials, the existence of interfaces gives rise to interfacial polarization or the Maxwell-Wagner-Sillers (MWS) effect. This effect appears in heterogeneous media because of the accumulation of charges at the interfaces. Nevertheless, this polarization is why the dielectric permittivity becomes high at low frequencies and high temperatures. To overcome the difficulty of observing the interfacial polarization, the modulus formulism can be used to analyze the electrical conductivity in an ionic polymeric material. In addition, the modulus formalism can be used to suppress the signal intensity associated with the electrode polarization, emphasizing the small features at high frequencies. The recorded dielectric data can be expressed in terms of the complex electric modulus (M^*), which is defined as the inverse of the complex permittivity (ε^*):

$$M^* = \frac{1}{\varepsilon^*} = \frac{\varepsilon'}{\varepsilon'^2 + \varepsilon''^2} + i\frac{\varepsilon''}{\varepsilon'^2 + \varepsilon''^2} \quad (3)$$

or $$M^* = M' + iM'' \quad (4)$$

where M' and M'' are the real and imaginary parts of the electric modulus, respectively.

Figure 6(a-c) shows the temperature dependence of M' for pure PVC, and Cr_2O_3-doped PVC films at different frequencies. It is clear that the values of M' decrease with increasing temperatures and increasing Cr_2O_3 content. At high temperatures, $M'(T)$ tends to reach a constant value, which indicates thermally activated nature of the dielectric constant [35]. The Cr_2O_3 nanoparticles within the PVC matrix influence the polarization and correspondingly the electrical conductivity and dielectric permittivity.

The temperature-dependent behavior of M'' for pure PVC and PVC loaded with Cr_2O_3 nanoparticles at selected frequencies is displayed in Figure 7(a-c). Pure PVC, and nanocompsite films exhibit a peak around T = 370 K consistent with the inflection temperature in $M'(T)$ curves (see Figure 6). It can be attributed to α_a-relaxation which ascribed to the micro-Brownian motion of the polymer main chains [18]. This peak becomes broad and shifts to higher temperature either with increasing frequency or increasing the content of Cr_2O_3 nanoparticles. In addition, an enhancement of the contribution of dc conductivity effects can be seen by using the electric modulus formalism. It noticed that the height of this peak for pure PVC film is higher than those of the nanocomposite films. The low-frequency side of this peak signifies the range of frequencies in which ions can successfully hop to neighboring sites. The high-frequency side of this M'' peak represents the range of frequencies in which the ions are spatially confined to their potential wells and only show localized motion within the well. Thus, the region where the peak occurs is indicative of the transition from long-range to short range mobility with increasing frequency. In addition, the spectrum of M'' might indicate that the conduction mechanism is temperature-dependent hopping [36].

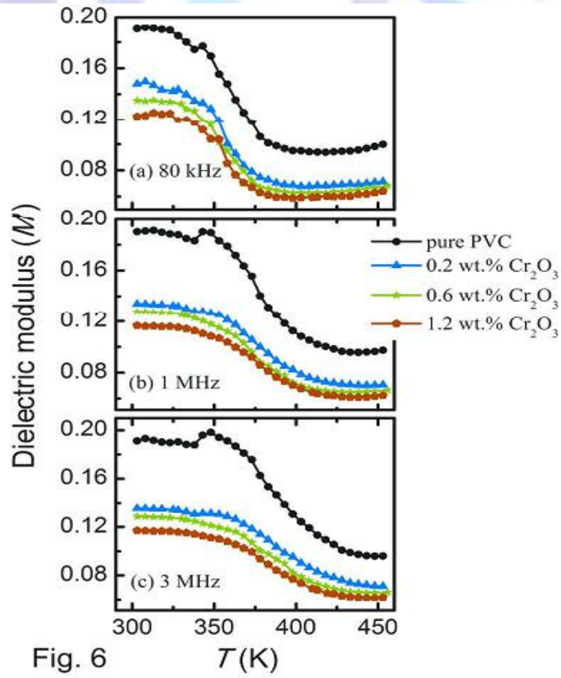

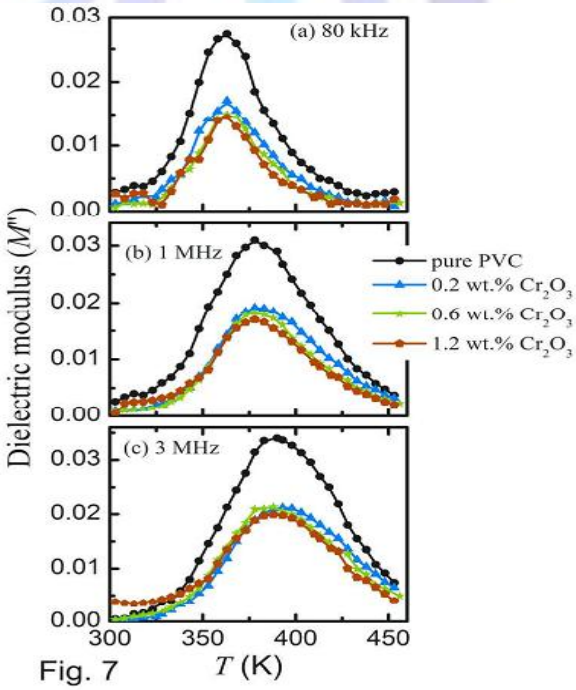

FIG. 6: Temperature dependence of the real part of the electric modulus, *M′*, for pure PVC and PVC containing different ratios of Cr_2O_3 nanoparticles at various frequencies: (a) 80 kHz , (b) 1 MHz K and (c) 3 MHz.

FIG. 7: Temperature dependence of the real part of the electric modulus, *M″*, for pure PVC and PVC containing different ratios of Cr_2O_3 nanoparticles at various frequencies: (a) 80 kHz , (b) 1 MHz K, and (c) 3 MHz.

OPTICAL PROPERTIES

UV-vis absorption spectroscopy is a direct and simple method to probe the band structure of samples. The UV-vis absorption spectra of pure PVC and PVC loaded with Cr_2O_3 nanoparticles are presented in Figure 8(a). The absorbance of the films increases with increasing Cr_2O_3 content in the PVC matrix. An absorption band at ~278 nm is observed for pure PVC and assigned to the π–π* transition [37, 38]. The intensity of this band increases in the spectra of the PVC/Cr_2O_3 nanocomposite films, as shown in the inset of Figure 8(a). Similar behavior was also observed for zinc oxide (ZnO)/PVC nanocomposites [39]. Two peaks around 440 and 550 nm are observed for the Cr_2O_3-doped PVC films, consistent with the spectra obtained for 0.75 *wt.*% Cr_2O_3-doped polyvinyl alcohol [28], in which these peaks were attributed to the formation of charge transfer complexes. Figure 8(b), reveals that PVC is an optically transparent polymer with transmission (*T*) over 90% in the visible region. The transmittance intensity of PVC increases with wavelength. As the concentration of Cr_2O_3 nanoparticles increases, the transmittance of the films decreases. The reduced transmittance is caused by the Cr_2O_3 nanoparticles increasing the localized state density or acting as scattering centers in the PVC matrix. The regular change in both the absorbance and transmittance of the nanocomposite films with Cr_2O_3 content provides evidence for the good dispersion of Cr_2O_3 nanoparticles in the PVC matrix, consistent with SEM results.

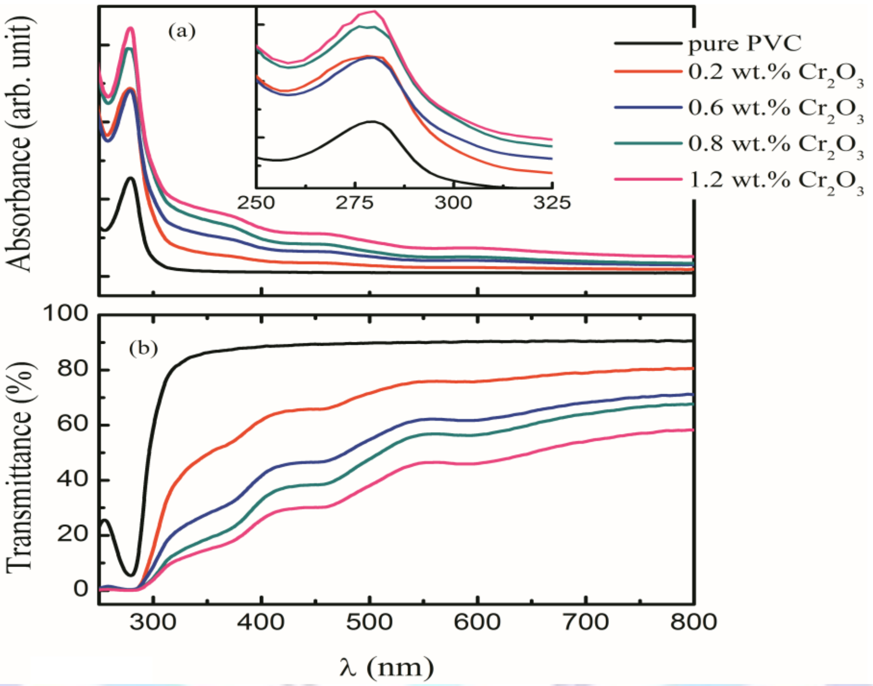

FIG. 8: (a) UV-vis absorption spectra, and (b) transmittance spectra of pure PVC, and PVC/Cr_2O_3 nanocomposite films. For clarity, the inset in (a) shows the change in the absorption spectra of all samples around 278 nm.

The direct optical energy band gap (E_g) of the films was determined from their UV-vis spectra according to the frequency dependence of the absorption coefficient, α, (where α= absorbance/film thickness) and by using Tauc's relation [8, 30, 40, 41]:

$$\alpha h\upsilon = B\left(h\upsilon - E_g\right)^r \quad (5)$$

where $h\upsilon$ is the incident photon energy that can be approximated to $h\upsilon$ = 1240/λ, B is a constant between 1 × 10^5 and 1 × 10^6 (cm eV)$^{-1}$[42, 43], and r is assumed to be 1/2 or 2 for allowed direct and allowed indirect transitions, respectively [44]. A plot of $(\alpha h\upsilon)^2$ versus $h\upsilon$ at *RT* enables us to estimate E_g by extrapolating the linear part of $(\alpha h\upsilon)^2$ to zero, as shown in Figure 9(a). The obtained E_g values are listed in Table 2. For pure PVC, E_g= 5.08 eV, which is similar to that reported in Ref. [45]. E_g decreased to 4.66 eV as the Cr_2O_3 content increased to 1.2 *wt.*%. Similar behavior has been reported for other composite polymers [14, 46, 47]. The decrease in E_g is attributed to the creation of localized states in the band gap as a result of Cr_2O_3 doping.

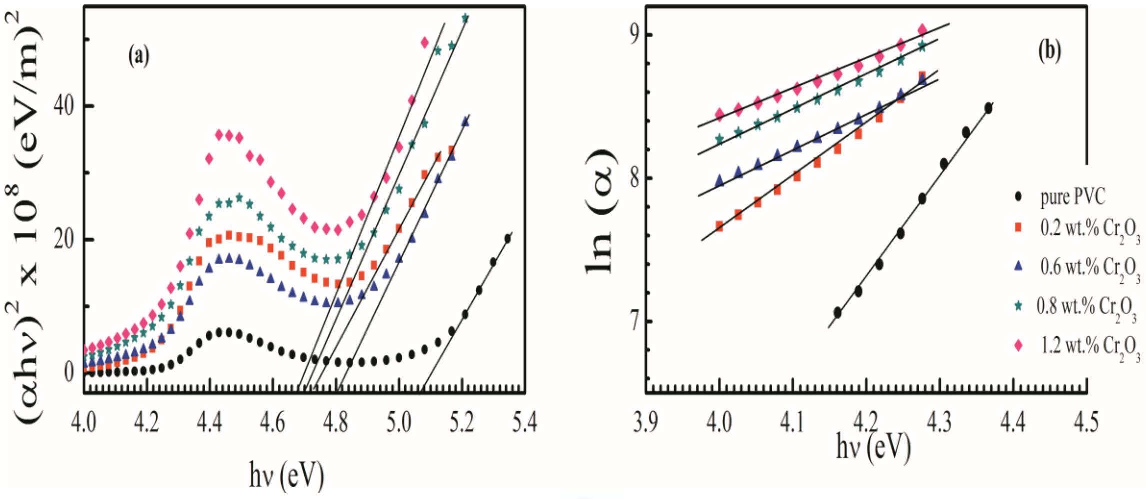

FIG. 9: (a) Plots of $(\alpha h\nu)^2$ versus *hv* and (b) *ln (α) vs. hv* of pure PVC and Cr_2O_3/PVC nanocomposite films. The solid lines in b are the fittings according to Eq. (6).

The absorption coefficient near the fundamental absorption edge depends exponentially on *hυ* and obeys the empirical Urbach relation. The Urbach energy (E_U) can be calculated using the following equation [48]:

$$\alpha = \alpha_o \exp(\frac{h\upsilon - E_I}{E_U}) \qquad (6)$$

where E_I and α_o are constants. E_U values were calculated from the slopes of the graphs in Figure 9(b) using the relationship $E_U = (\frac{dln\alpha}{dh\upsilon})^{-1}$, and are given in Table 2. The E_U values of the PVC films increased with Cr_2O_3 content. E_U changed inversely to E_g, which may be caused by the disorder of the PVC matrix being increased by Cr_2O_3 doping. This increase leads to a redistribution of states from band to tail, allowing a large number of possible band-to-tail and tail-to-tail transitions [49]. Moreover, the decrease in the optical band gap, E_g, and the increase of σ_{ac} reveal the consistency between the ac conductivity and optical measurements.

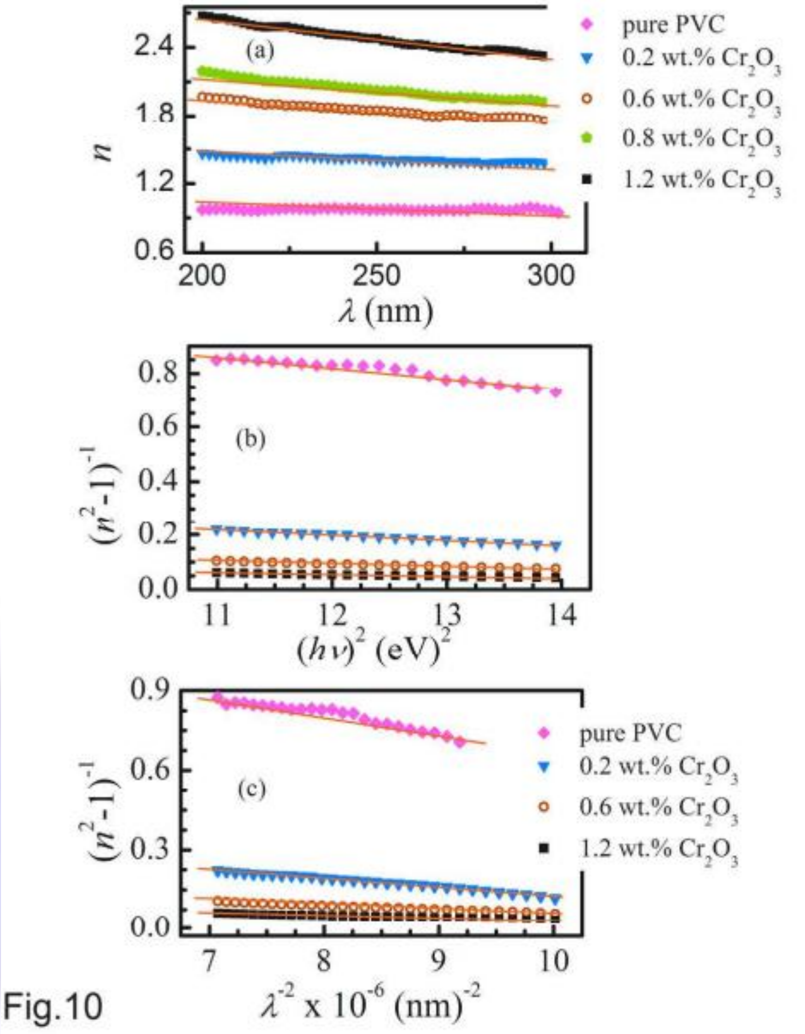

FIG. 10: (a) Dependence of refractive index (*n*) on wavelength (*λ*).Plots of (b) *$(n^2\text{-}1)^{-1}$* against *$(h\nu)^2$*, and (c) *$(n^2\text{-}1)^{-1}$* versus *λ^{-2}* for pure PVC and PVA/Cr_2O_3 nanocomposite films. The solid red lines in b and c are the linear fitting according to Eqs. 8 and 9, respectively.

One of the methods to calculate the refractive index (*n*) is using the reflectance (*R*) and extinction coefficient, *k*, (*k* = *αλ/4π*) of films [50]:

$$n = [4R/(1-R)^2 - k^2]^{1/2} + [(1+R)/(1-R)] \quad (7)$$

where *n* is the real part of the complex refractive index given by $\tilde{n} = n + ik$, and *R* is the reflectance calculated from the absorbance (*A*) and transmission (*T*) spectra using the relation; $R = 1 - [T * \exp(A)]^{1/2}$ [18,50]. Figure 10(a) shows the refractive index distributions of the pure PVC film and the PVC films loaded with Cr_2O_3 nanoparticles. *n* in the visible region for the pure PVC film is 1.48, which is consistent with values measured for PVC with an Abbe's refractometer and thermostat-controlled water circulation system at 30 °C by Rajulu *et al*. [51]. Figure 10(a) reveals that *n* of the nanocomposite films increased markedly upon incorporation of Cr_2O_3 nanoparticles into the PVC matrix, similar to PVC/CdO nanocomposites [17]. The physical properties of a material depend strongly on its internal structure, including packing density and molecular weight distribution. The increased *n* of PVC after embedding Cr_2O_3 nanoparticles may be caused by the formation of intermolecular hydrogen bonds between the oxygen atoms of Cr_2O_3 and the adjacent hydrogen atoms of PVC. Such increases in *n* may allow these materials to be used as an anti-reflection coating for solar cells, or as high-refractive-index lenses.

ISSN: 2347-3487

TABLE 2: Optical parameters of pure PVC and PVC loaded with Cr_2O_3 nanoparticles. Listed are: direct energy band gap (E_g), Urbach energy (E_U),), single oscillator energy (E_o), energy parameter (E_d), transmittance (T%), refractive index at infinite wavelength (n_∞), average interband oscillator wavelength (λ_o), average oscillator strength (S_o), lattice dielectric constant (ε_1) and the ratio between carrier concentration and effective electron mass ($Ne^2/\pi c^2 m^*$).

Sample	Pure PVC	0.2 *wt.*% Cr_2O_3	0.6 *wt.*% Cr_2O_3	0.8 *wt.*% Cr_2O_3	1.2 *wt.*% Cr_2O_3
E_g (eV)	5.06	4.74	4.84	4.70	4.66
E_U (eV)	0.137	0.271	0.403	0.433	0.487
E_o (eV)	4.47	3.25	3.35	3.18	3.12
E_d (eV)	5.20	15.22	30.47	39.73	51.93
T % (at 500 nm)	89.8	71.6	54.7	47.7	38.0
n_∞	1.47	2.36	3.05	3.67	4.20
λ_o (nm)	274	377	353	381	390
S_o x 10^{13} (m^{-2})	1.53	3.16	6.68	8.61	10.95
ε_1	2.0	2.95	3.95	4.40	5.40
($Ne^2/\pi m^* c^2$) × 10^{-7} (nm^{-2})	3.60	11.22	26.98	39.89	47.45

From the normal dispersion behavior of n with λ, various dispersion parameters can be calculated within the absorbance band (200–300 nm) on the basis of the single oscillator model developed by DiDomenico and Wemple [52,53]:

$$n^2 = 1 + \frac{E_d E_o}{E_o^2 - (h\upsilon)^2} \qquad (8)$$

where E_d is the energy parameter (a measure of the strength of interband optical transitions) and E_o is the single oscillator energy (the average excitation energy for electronic transitions). E_d and E_o can be obtained from the intercept and slope of the linear fitted line in a plot of $(n^2-1)^{-1}$ against $(hv)^2$, as depicted in Figure 10(b). The determined values of E_d and E_o are listed in Table 2. The variation of n with λ can be expressed as [54]:

$$\frac{n_\infty^2 - 1}{n^2 - 1} = 1 - (\frac{\lambda_o}{\lambda})^2 \qquad (9)$$

where n_∞ is the long-wavelength refractive index and λ_o is the average interband oscillator wavelength. The parameters n_∞, λ_o, and S_o (average oscillator strength; $S_o = (n_\infty^2 - 1)/\lambda_o^2$) were obtained from the slope and intercepts of $(n^2\text{-}1)^{-1}$ versus λ^{-2} curves, as presented in Figure 10(c). The values of these parameters are also given in Table 2. The optical parameters of PVC are changed by the incorporation of Cr_2O_3 nanoparticles into the PVC matrix. This suggests that the optical constants of the nanocomposite films could be controlled by Cr_2O_3 content. The quantitative measurements of these parameters may assist in tailoring and modeling the properties of such nanocomposites for use in optical components and devices.

ISSN: 2347-3487

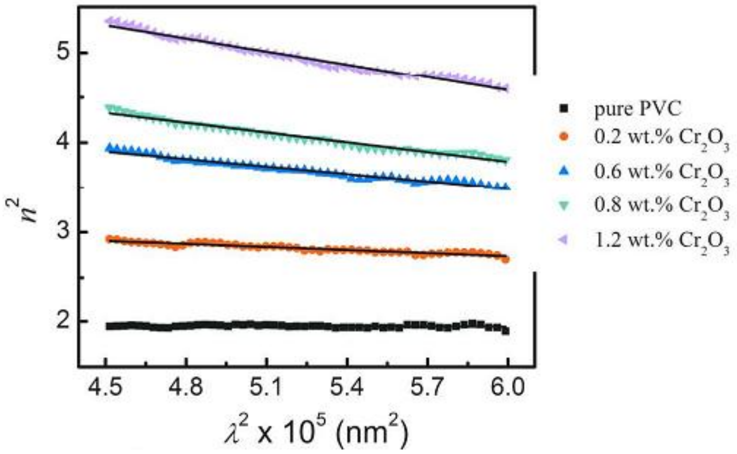

FIG. 11: Dependence of (n^2-1)$^{-1}$ on λ^2 for pure PVC and Cr_2O_3-doped PVC films. The solid lines are the fitting according to Eq. (10).

The lattice dielectric constant (ε_1) and ratio of carrier concentration to electron effective mass ($e^2/\pi c^2$)(N/m^*) can be calculated (see Table 2) by plotting the variation of n^2 *versus* λ^2 (Figure 11) according to the dispersion relation [1]:

$$n^2 = \varepsilon_1 - \left(\frac{e^2}{\pi c^2}\right)\left(\frac{N}{m^*}\right)\lambda^2 \qquad (10)$$

Table 2 reveals that the values of ($e^2/\pi c^2$)(N/m^*) increase with Cr_2O_3 content. This means that Cr_2O_3 incorporation increases the charge carrier concentration inside the PVC matrix.

The real and imaginary parts of complex dielectric constants can be calculated from the following relations [55]:

$$\varepsilon_{real} = n^2(\lambda) - k^2(\lambda) \qquad (11)$$

$$\varepsilon_{imag.} = 2k(\lambda)\, n(\lambda) \qquad (12)$$

where ε_{real} and $\varepsilon_{imag.}$ are calculated for pure PVC and PVC containing different amounts of Cr_2O_3 nanoparticles at different incident photon energies. Fig. 12(a) and (b) show that as incident photon energy increases ε_{real} and ε_{imag} increased and then peaked at certain energies ($h\nu$ ~4.45 eV). The 1.2 *wt.%* Cr_2O_3-doped composite film has the largest ε_{real} and $\varepsilon_{imag.}$ of the films over a wide energy range.

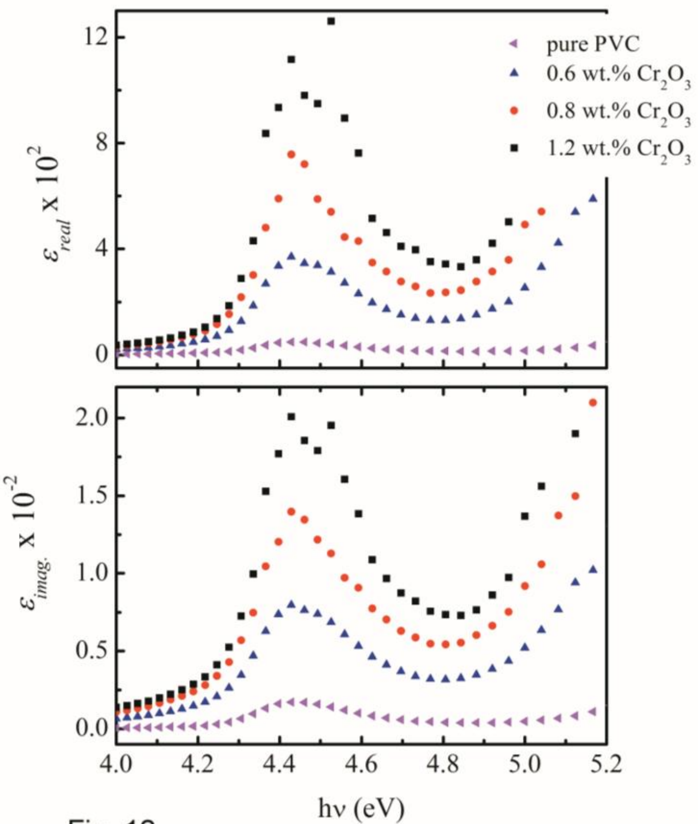

FIG. 12: Plots of (a) the real part (ε_{real}), and (b) the imaginary part ($\varepsilon_{imag.}$) of the optical dielectric constant versus photon energy $h\nu$ for pure PVC and PVC doped with Cr_2O_3 nanoparticles.

CONCLUSIONS

Rietveld XRD analysis indicated that the as-prepared Cr_2O_3 nanoparticles were rhombohedral with space symmetry group $R\bar{3}c$. The increase in the dielectric permittivity of Cr_2O_3-doped PVC films is attributed to the interfacial polarizations. The frequency and temperature dependences of the ac conductivity for the investigated nanocomposite films indicated that the charge carriers are transported by hopping through defect sites along the PVC chains. The electric modulus *M*" showed α_a-relaxation due to the micro-Brownian motion of the polymer main chains. Adding the Cr_2O_3 nanoparticles to PVC films modified their optical properties considerably. The direct optical energy band gap showed a red shift from 5.08 to 4.66 eV upon addition of Cr_2O_3 nanoparticles. The refractive index of pure PVC is increases with Cr_2O_3 content. Optical dispersion constants also change. The real and imaginary parts of dielectric constants for pure PVC exhibit a peak at $h\nu$ ~4.45 eV and the intensity of this peak is enhanced with Cr_2O_3 doping. These results reveal that PVC/Cr_2O_3 nanocomposite films may be suited for application in optical devices.

ACKNOWLEDGMENTS

The assistance of Prof. Dr. A. Krimmel, University of Augsburg, Germany for the Rietveld XRD refinement is gratefully acknowledged.

References

1. Chahal, R.P., Mahendia, S., Tomar, A.K., and Kumar, S. J. 2012. Alloys Compd. 538, 212.
2. Wu, W., Liang, S., Shen, L., Ding, Z., Zheng, H., Su, W., and Wu, L. 2012. J. Alloys Compd., 520, 213.
3. Zare, Y. 2013. Waste Manage. 33, 598.
4. Cho, S., and Choi, W. 2001. J. Photochem. Photobiol. A: Chem., 143, 221.
5. Fang, L., Song, Yi-h., Zheng, Xiao-n., Chen, Shao-h., Da, Pei-h., and Zheng, Q. 2010. Chinese J. Polym. Sci., 28, 637.
6. Yoo, H., and Kwak, S.-Yeop. 2011. Appl. Catal. B Environ., 104, 193.
7. Liu, F., Liu, H., Li, X., Zhao, H., Zhu, D., Zheng, Y., and Li, C. 2012. Appl. Surf. Sci., 258, 4667.

8. Reddeppa, N., Sharma, A.K., Rao, V.V.R.N., and Chen, W. 2013. Microelectron. Eng., 112, 57.
9. Al-Hartomy, O.A., Al-Salamy, F., Al-Ghamdi, A.A., Abdel Fatah, M., Dishovsky, N., and El-Tantawy, F. 2011. J. Appl. Polym. Sci., 120, 3628.
10. Al-Ghamdi, A.A., El-Tantawy, F., Abdel Aal, N., El-Mossalamy, E.H., and Mahmoud, W.E. 2009. Polym. Degrad. Stab., 94, 980.
11. Mahmoud, W.E., and Al-Ghamdi, A.A. 2011. Polym. Compos., 32, 1143.
12. El ashmawi, I.S., Hakeem, N.A., Marei, L.K., and Hanna, F.F. 2010. Phys. B, 405, 4163.
13. Olad, A., and Nosrati, R. 2013. Prog. Organ. Coat., 76, 113.
14. Ma, F., Yuan, N., and Ding, J. 2013. J. Appl. Polym. Sci., 128, 3870.
15. Kemal, I., Whittle, A., Burford, R., Vodenitcharova, T., and Hoffman, M. 2013. J. Appl. Polym. Sci., 127, 2339.
16. Sterzynski, T., Tomaszewska, J., Piszczek, K., and Skórczewska, K. 2010. Compos. Sci. Technol., 70, 966.
17. El Sayed, A.M., El-Sayed, S., Morsi, W.M., Mahrous, S., and Hassen, A. Polym. Compos. DOI: 10.1002/pc.22839, in press.
18. El Sayed, A.M., and Morsi, W.M. 2013. Polym. Compos., 34, 2031.
19. Medeiros, A.M.L., Miranda, M.A.R., de Menezes, A. S., Jardim, P. M., da Silva, L.R.D., Gouveia, S.T., and Sasaki, J.M.J. 2004. Metastable, nanocryst. Mater., 20-21, 399.
20. Farzaneh, F., and Najafi, M. 2012. J. Sci. Islamic Republi c of Iran, 22, 329.
21. Kim, D.-W., and Oh, S.-G. 2005. Mater. Lett., 59, 976.
22. Yu-Feng, Z., Zheng-Song, L., and Qian-Wang, C. 2004. Chin. J. Inorg. Chem., 20, 8, 971.
23. Pei, Z., Xu, H., and Zhang, Y. 2009. J. Alloys Comp., 468, L5–L8.
24. Pei Z., and Zhang, Y. 2008. Mater. Lett., 62, 504.
25. Wang, Y., Yuan, X., Liu, X., Ren, J., Tong, W., Wang, Y., and Lu, G. 2008. Sol. Stat. Sci., 10, 1117.
26. Hill, A.H., Harrison, A., Dickinson, C., Zhou, W., and Kockelmann, W. 2010. Micropor, Mesopor., Mat., 130, 280.
27. Makhlouf, S. A., Bakr, Z. H., Al-Attar, H., and Moustafa, M.S. 2013. Mater. Sci. Eng. B, 178, 337.
28. Hassen, A., El Sayed, A.M., Morsi, W.M., and El-Sayed, S. 2012. J. Appl. Phys., 112, 093525.
29. Mahmoud, W.E., Hafez, M., El-Aal, N.A., and El-Tantawy, F. 2008. Polym. Int., 57, 35.
30. Mahmoud, W.E. 2011. Euro. Polym. J., 47, 1534.
31. Kyritsis, A., Pissi, P., and Grammatikakis, I. 1995. J. Polym. Sci. Part B: Polym. Phys., 33, 1737.
32. Rao, V., Ashokan, P.V., and Shridhar, M.H. 2000. Mater. Sci. Eng., A281, 213.
33. Migahed, M.D., Ishra, M., Fahmy, T., and Barakat, A. 2004. J. Phys. Chem. Solids, 65, 1121.
34. Saqan, S.A., Ayesh, A.S., Zihlif, A.M., Martuscelli, E., and Ragosta, G. 2004. Polym. Test., 23, 739.
35. Jonscher, A.K. Dielectric Relaxation in Solids, Chelsea Dielectrics Press, London 1983.
36. Tsangaris, G.M., Kouloumbi, N., and Kyvelidis, S. 1996. Mater. Chem. Phys., 44, 245.
37. Allen, N.S., Edge, M., Rodriguez, M., Liauw, C.M., and Fontan, E. 2000. Polym. Degrad. Stab., 68, 363.
38. Giuffrida, S., Condorelli, G.G., Costanzo, L.L., Ventimiglia, G., Mauro, A.D., and Fragal, I. L. 2008. J. Photochem. Photobiol. A: Chem., 195, 215.
39. Al-Taa'y, W., Abdul Nabi, M., Yusop, R.M., Yousif, E., Abdullah, B.M., Salimon, J., Salih, N., and Zubairi, S.I. 2014. Int. J. Polym. Sci. 2014, Article ID 697809, 6 pages http://dx.doi.org/10.1155/2014/697809
40. Mahmoud, W.E., Al-Ghamdi, A.A., and Al-Agel, F. 2011. Polym. Advan. Technol., 22, 2055.
41. Mahmoud, W.E., Shirbeeny, W., Al-Ghamdi, A.A., and Al-Heniti, S., 2012. J. Appl. Polym. Sci., 125, 339.
42. Dutta, M., Mridha, S., and Basak, D. 2008. Appl. Surf. Sci., 254, 2743.
43. Keskenler, E.F., Turgut, G., and Dogan, S. 2012. Superlatt. Microstruc., 52, 107.
44. Wen, R., Wang, L., Wang, X., Yue, G.H., Chen, Y., and Peng, D.L. 2010. J. Alloys Compd., 508, 370.
45. Ahmed, A., Najim, T., Salimon, J., Salih, N., Graisa, A., Farina, Y., and Yousif, E. 2010. ARPN J. Eng. Appl. Sci., 5, 43.
46. Mohan, K.R., Achari, V.B.S., Rao, V.V.R.N., and Sharma, A.K. 2011. Polym. Test., 30, 881.

47. Sekhar, P.C., Kumar, P.N., Sasikala, U., Rao, V.V.R.N., and Sharma, A.K. 2012. Eng. Sci. Technol. In. J. (ESTIJ), 2, 908.
48. Urbach, F. 1953. Phys. Rev., 92, 1324.
49. O'Leary, S.K., Zukotynski, S., and Perz, J.M. 1997. J. Non-Cryst. Solids, 210, 249.
50. Yahia, I.S., Farag, A.A.M., Cavas, M., and Yakuphanoglu, F. 2013. Superlatt. Microstruc., 53, 63.
51. Rajulu, A.V., Reddy, R.L., Raghavendra, S.M., and Ahmed, S.A. 1999. Eur. Polym. J., 35, 1183.
52. Sellmeier, W. 1871. Ann. Phys. Chem., 143, 271.
53. Wemple, S.H., and DiDomenico, M. 1970. Phys. Rev., B3, 1338.
54. Zheng, B.J., Lian, J.S., Zhao, L., and Jiang, Q. 2010. Appl. Surf. Sci., 253, 2910.
55. Al-Ghamdi, A.A. 2006. Vacuum, 80,400.

Authors' biography

1. A. Hassen

A. Hassen received Ph.D. in Natural Science from Faculty of Science and Mathematics, University of Augsburg, Germany in 2003. He was awarded postdoctoral scholarships from Indian National Science Academy in 2005 and South Korea (BK21 projct), Pusan National University in 2007. He is an Associate Professor in the Department of Physics, Faculty of Science, Fayoum University, Egypt and Taif University, KSA since 2009. He has published many papers in international peer-reviewed journals and conferences. For the research works, he has won several awards/prizes from Taif and Fayoum Universities. He is a reviewer for several international journals. He is an Associate Editor for two international Journals. His main research area is polymer composites/nanocomposites, characterization of materials, superconducting materials, peroveskite manganites and cobaltites, and structure-properties relationship etc.

2 . S. El-Sayed

S. El-Sayed obtained M.Sc. in polymer composites from Faculty of Science, Cairo University, Egypt in1996. She received Ph.D in polymer physics from Faculty of Science, Cairo University, Egypt in 2003. She has worked as a lecturer in Fayoum university from 2003 to 2007. She is the head of Physics Department, Faculty of Science and Education (for Girls), Taif University, Saudi Arabia since 2009. She has published many papers in international journals. She is a reviewer for different international Journals. Her interesting research area is polymer physics, polymer composite/ nanocomposites.

3. W.M. Morsi

Wafaa M. Morsi obtained PhD in Experimental Physics from Department of Physics, Cairo University, Egypt in 2011. She worked as a Researcher in Building Physics Institute, Housing& Building National Research Center, Egypt. She has published about 6 papers in national and international journals and conferences. She is a researcher in many research project. Her interesting research area is nano-composites, microstructure and physical properties.

4. Adel El Sayed (A.M. El Sayed)

Adel El Sayed obtained M.Sc. in Experimental Solid State Physics, from Physics department, Faculty of Science, Fayoum University, in 2008. Thesis entitled " Influence of Laser Irradiation on the Physical Properties of some Solid State Nuclear track Detectors". He obtained PhD in Experimental Solid State Physics, from Physics department, Faculty of Science, Fayoum University, in 2011. Thesis entitled "Characterization of some TM-doped ZnO Synthesized via Chemical Deposition". Now he is a lecturer at Physics Department, Faculty of Science. He has published some papers of radiation effects on polymers, polymer nanocomposites, and thin films of transition metals (TM) oxides.